Extreme Mechanics Letters 40 (2020) 100891

Contents lists available at ScienceDirect

Extreme Mechanics Letters

journal homepage: www.elsevier.com/locate/eml

Topological adhesion II. Stretchable adhesion

Jiawei Yang [a,1], Jason Steck [a,1], Ruobing Bai [b], Zhigang Suo [a,*]

[a] John A. Paulson School of Engineering and Applied Sciences, Kavli Institute for Bionano Science and Technology, Harvard University, Cambridge, MA 02138, USA
[b] Division of Engineering and Applied Science, California Institute of Technology, Pasadena, CA, 91125, USA

ARTICLE INFO

Article history:
Received 22 June 2020
Received in revised form 15 July 2020
Accepted 15 July 2020
Available online 22 July 2020

Keywords:
Topological adhesion
Chitosan
pH
Stretchable interface
Adhesion energy

ABSTRACT

When two stretchable materials (e.g., hydrogels, elastomers, and biological tissues) are adhered, the interface should be stretchable, without constraining the deformation and degrading adhesion. Here we develop methods to characterize stretchable adhesion. We do so by topological adhesion, using polyacrylamide hydrogels as adherends, chitosan as stitch polymers, and a change in the pH as a trigger. We prestretch the topohered hydrogels in several ways, and measure adhesion energy when the hydrogels are either in the un-stretched or the stretched state. Stretchable adhesion is achieved when the adhesion energy can maintain a similar level, insensitive to the prestretch. We study the mechanism of stretchable adhesion formed by the chitosan topohesive.

Adhesion is widely practiced in industry, medicine, and daily life [1,2]. Adhesion is traditionally performed on dry and hard materials, such as glasses, ceramics, plastics, and metals. These materials typically only sustain small deformation, and so does the interface. By contrast, stretchable materials are usually required to sustain large deformation. A non-stretchable interface limits the deformation of soft materials, and a stretch in the plane of the interface may degrade adhesion.

Acrylic, silicone, polyurethane, poly(vinyl acetate), epoxy, and cyanoacrylate are among the most commonly used to adhere hard materials [3]. These liquid-form adhesives wet the interface of two adherends and cure into a dense glassy polymer layer. Strong adhesion is formed through the densely packed non-covalent interactions between the glassy polymer layer and the surfaces of the two adherends [4,5]. The legendary "super glue", cyanoacrylate, has been recently used to adhere elastomers, hydrogels, and tissues [6–8]. Upon curing, the glassy polycyanoacrylate layer forms dense topological entanglement with the two polymer networks of the adherends. However, the continuous glassy layer is non-stretchable, which hardens the interface and makes the interface translucent or even opaque [6,9]. The glassy layer easily fractures into several fragments under stretch. The edges of the fragments can concentrate strain, rupture the nearby polymer chains, and lead to damage of the adherends (Fig. 1a). By contrast, when a layer of sparse and strong interlinks connects two soft materials at the interface, a stretch parallel to the interface deforms polymer chains between two interlinks but does not rupture them; upon removing the stretch, the deformed polymer chains relax and restore their initial configurations (Fig. 1b). Such interface is stretchable. The stretchable adherends and their interface remain intact during the deformation, and the adhesion can be stretchable.

The above pictures provide an ample design space of molecular topologies to realize stretchable adhesion. Examples include a layer of bridge polymers [10] (Fig. 2a), a stitch polymer network [11] (Fig. 2b), and a layer of sparse glassy islands [8] (Fig. 2c). Recently developed soft integrated devices leverage strong and stretchable adhesion to display many novel functions in engineering and medical applications [4,12–15], such as artificial muscles [16,17], skins [18,19], axons and textiles [20,21], ionic conductors [22,23], touchpads [24], diodes [25], and luminescence [26,27], stretchable and interactive seals [28,29], wound dressing [6,10], tissue repair [10,30,31], medical implants [32,33], medical device coating [34,35], and drug delivery [36,37].

The rapidly developing interest in stretchable adhesion poses a question: How should stretchable adhesion be characterized? Here we characterize stretchable adhesion in two ways: (i) the adhered materials are prestretched monotonically or cyclically, and the adhesion energy is measured while the materials are in the un-stretched state; (ii) the adhered materials are prestretched for a period of time, and the adhesion energy is measured while the materials are in the stretched state. Stretchable adhesion is achieved when the adhesion energy maintains a similar level, insensitive to the prestretch, the types of adhered materials, and the mechanical properties of adhered materials, so long as the adhered materials are as stretchable as one requires.

* Corresponding author.
E-mail address: suo@seas.harvard.edu (Z. Suo).
[1] There authors contribute equally to this work.

https://doi.org/10.1016/j.eml.2020.100891
2352-4316/

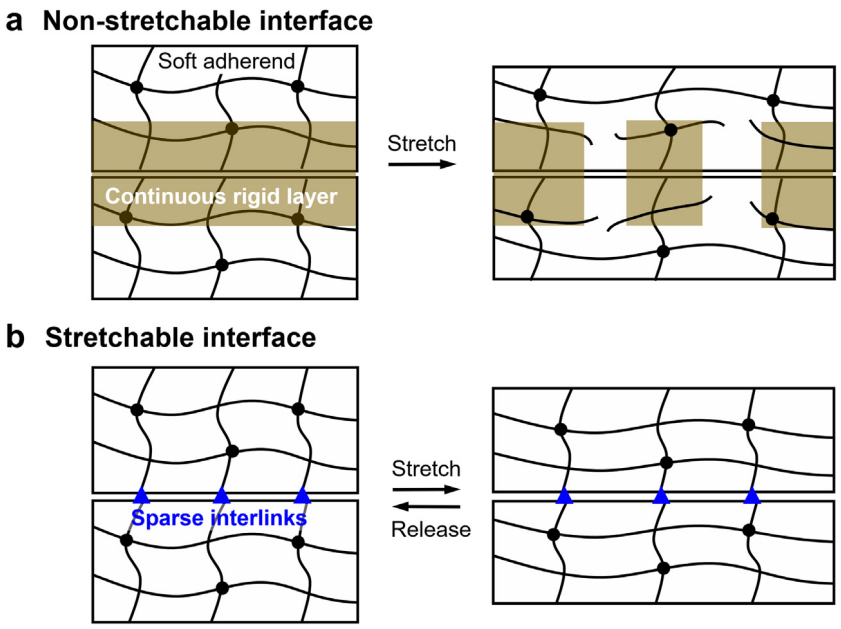

Fig. 1. Non-stretchable and stretchable interfaces. a, When two stretchable materials are adhered by a continuous rigid layer, the interface is non-stretchable. Upon stretch, the rigid layer may fracture into several fragments, induce strain concentration at the edges, and lead to damage of the soft materials. **b**, When two stretchable materials are adhered by a layer of sparse and strong interlinks, the interface is stretchable. Upon stretch and release, the two materials and the interface deform reversibly without damage.

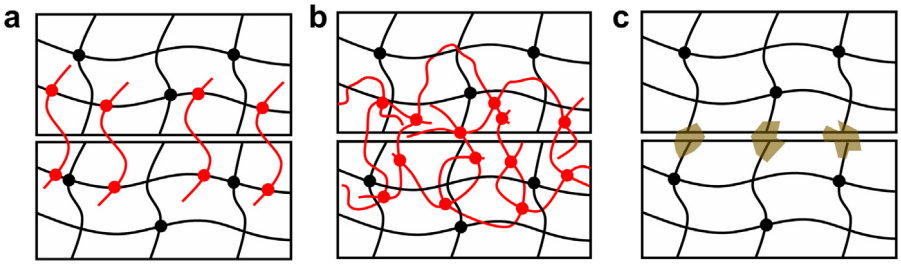

Fig. 2. Examples of molecular topologies that can enable stretchable adhesion. a, Bridge polymers, **b**, A stitch polymer network, and **c**, Sparse glassy islands.

We conduct experiments using a chitosan topohesive, as described in our previous paper [11]. Briefly, chitosan bears amine groups of pKa ∼6.5. When pH $<$ 6.5, the chitosan chains dissolve, and the solution becomes a viscous liquid (Fig. 3a). When pH $>$ 6.5, the chitosan chains form interchain hydrogen bonds and crosslink into a network, which precipitates as a solid (Fig. 3b). We prepare an aqueous solution of chitosan of pH = 5, and place it between two hydrogels of pH = 7 (Fig. 3c). The chitosan chains and H^+ diffuse into the two hydrogels concurrently. As H^+ dilutes (the diffusivity of H^+ is orders of magnitude higher than chitosan), the pH in the chitosan solution increases, such that the chitosan chains crosslink into a polymer network, in topological entanglement with the networks of the two hydrogels (Fig. 3d). Such topological entanglement is independent of the types and moduli of the hydrogels.

We prepare polyacrylamide hydrogels as adherends, and topohere them using the chitosan topohesive (Figure S1, see hydrogel preparation and procedure of adhesion in the supplementary information). The topohered hydrogels are subsequently stored in a sealed bag for 24 h to reach equilibrium in adhesion while maintaining their water content. We apply in-plane uniaxial stretch to the topohered hydrogels using an Instron tensile tester, with the stretch varying from 1 to 8. We next release the stretch and let the hydrogels return to the initial un-stretched state. At this un-stretched state, we attach inextensible backing layers to the hydrogels and immediately proceed to adhesion test (Fig. 4a and Figure S2, see detailed T-peeling test in the supplementary information). The adhesion energy is calculated as $\Gamma = 2F/W$, where F is the peeling force in the steady state and W is the width of the hydrogel. The results show that despite different stretch, even when the stretch is as large as 8, the adhesion energies all maintain a similar level above 200 J/m^2 (Fig. 4b). This adhesion energy approaches the fracture energy of the polyacrylamide hydrogels, which is measured to be about 450 J/m^2. This observation clearly shows that the topohered interface is stretchable against a single time of monotonic stretch. We next conduct cyclic stretch to the topohered hydrogels with a constant stretch amplitude of 2 and varied numbers of cycles from 1 to 10,000 (Figure S3, see experimental setup in the supplementary information). The adhesion energies still maintain a similar level above 200 J/m^2, for all numbers of cycles. This shows that the topohered interface is stretchable against cyclic stretch (Fig. 4c).

Adhesion should also be strong while the topohered hydrogels are being deformed. To characterize the adhesion in a stretched state, we prepare the same topohered hydrogels, apply a uniaxial stretch, and subsequently hold the stretch. At this stretched state, we attach the backing layers to the hydrogels to restrict the deformation, and immediately conduct the adhesion test (Fig. 5a). The adhesion energy is measured based on the deformed geometry, namely, $\Gamma = 2F/w$, where $w = W\lambda^{-1/2}$ is the width of the hydrogel under a uniaxial stretch λ. The adhesion energy decreases with the increase of the uniaxial stretch (Fig. 5b). The

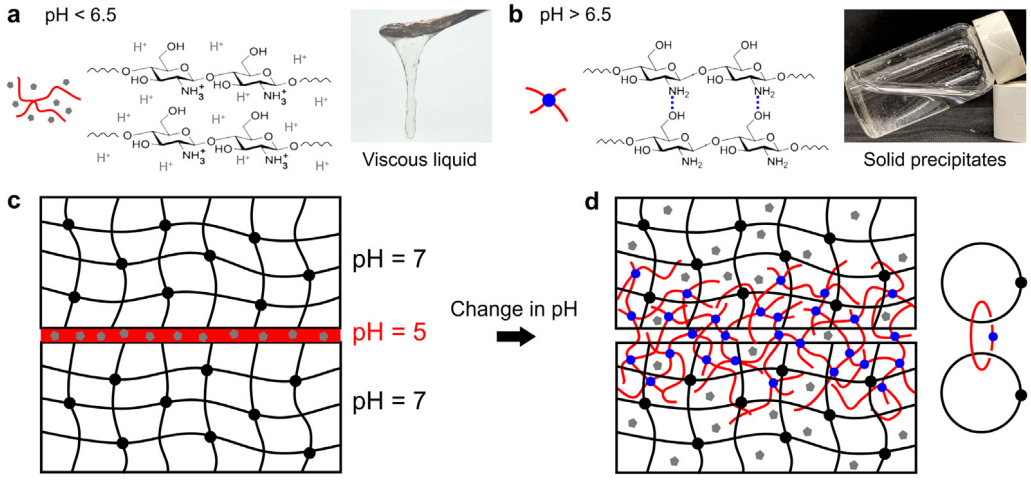

Fig. 3. Chitosan topohesive. a, Chitosan chains dissolve in aqueous solution and form a viscous liquid when pH < 6.5. b, Chitosan chains form a network through hydrogen bonds when the pH > 6.5. c, Two hydrogels of pH = 7 act as adherends, and chitosan chains act as stitch polymers. An aqueous solution of chitosan of pH = 5 is spread between two hydrogels. d, Both chitosan chains and H^+ diffuse into two hydrogels. As the concentration of H^+ in the chitosan solution decreases, the chitosan chains form a stitch network, in topological entanglement with the two hydrogel networks.

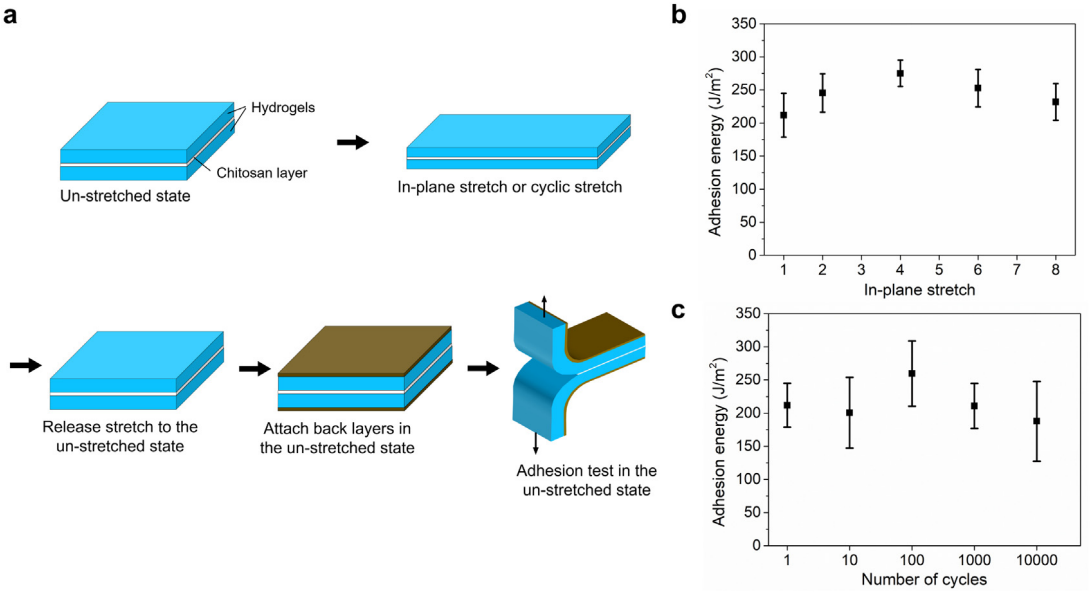

Fig. 4. Stretchable adhesion tested in the un-stretched state. a, Test procedure. b, Adhesion energy as a function of stretch. c, Adhesion energy as a function of number of cycles. The stretch amplitude is fixed at 2.

adhesion energy is measured to be ~100 J/m^2 at a stretch of 8, half of that measured with no stretch, but still shows fairly strong adhesion. We next apply a constant stretch of 4, hold that stretch for different period of time, and then perform the adhesion tests. The adhesion energy remains a similar level, about 150 J/m^2, independent of the hold time (Fig. 5c). The adhesion energies in the stretched state are lower than those in the un-stretched state. This difference may be attributed to a couple of factors, such as the rupture of some stitch chitosan network due to the large stretch, and the reduced energy dissipation from the hydrogels due to the break of short chains. How these factors affect the adhesion energy is uncertain at this writing and requires further study. Nonetheless, these results indicate that the topohered interface is strong even when it is stretched.

To understand the underlying mechanism of chitosan enabled stretchable adhesion, we first show that the chitosan topohesive does form a solid-like network during the topohesion. We employ scanning electron microscopy (SEM) to image the topohered interface of two polyacrylamide hydrogels. A chitosan layer is clearly observed, with a thickness of about 55 μm (Fig. 6a) (the initial thickness of chitosan solution spread at the interface is 222 μm). In addition, we also prepare a gelatin hydrogel and spread the chitosan topohesive on the hydrogel (See the preparation of gelatin hydrogel in the supplementary information). The chitosan–gelatin bilayer is optically transparent (Fig. 6b). Upon heating to about 50 °C, the gelatin hydrogel melts and becomes a viscous liquid, but the chitosan hydrogel should remain. Indeed, we are able to use a tweezer to pick up a solid film from the gelatin solution, which we expect to be the chitosan hydrogel (Fig. 6c).

We next explore the mechanical behavior of the formed chitosan gel in the topohesion. We spread a chitosan topohesive (pH = 5) on a polyacrylamide hydrogel (pH = 7), store for 24 h, and then conduct uniaxial tensile test to the chitosan–hydrogel bilayer. Before stretch, the surface of the chitosan–hydrogel bilayer is smooth. As the uniaxial stretch increases, we observe

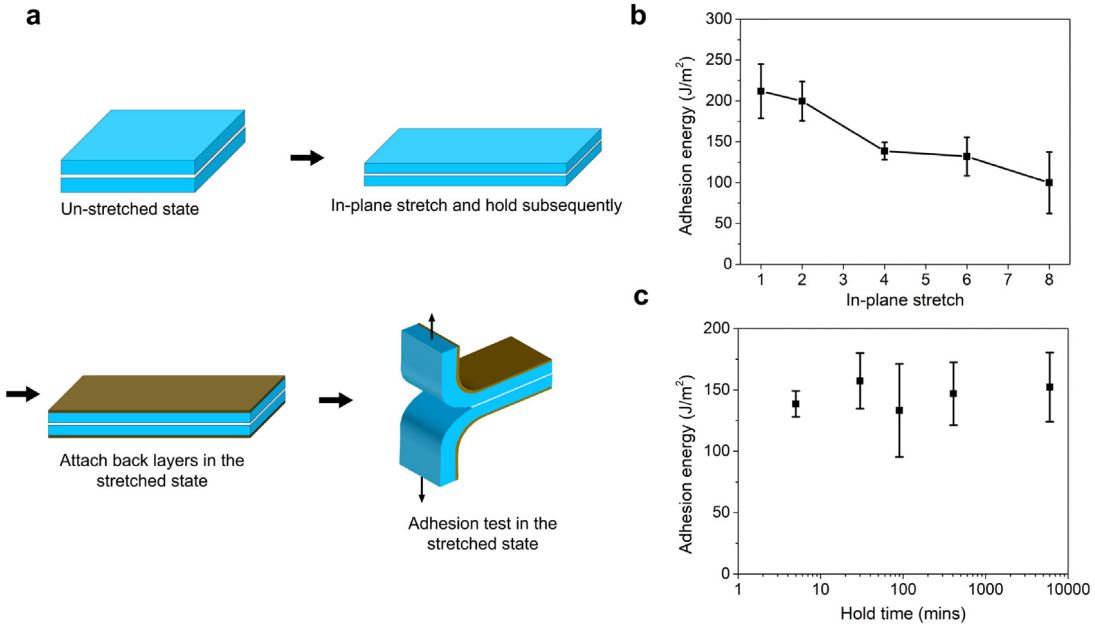

Fig. 5. Stretchable adhesion tested in the stretched state. a, Test procedure. b, Adhesion energy as a function of stretch. c, Adhesion energy as a function of hold time. The hold stretch is fixed at 4.

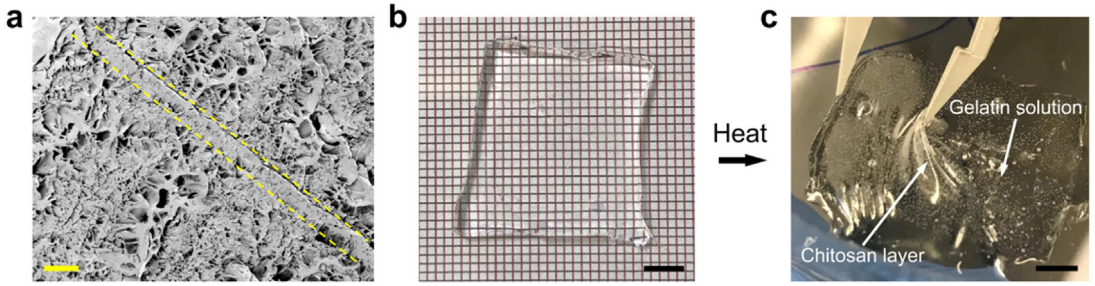

Fig. 6. Chitosan topohesive forms a solid hydrogel. a, Scanning electron microscope image shows the chitosan layer (enclosed by two yellow dash lines) between two polyacrylamide hydrogels. b, A chitosan solution is spread on a gelatin hydrogel. The entire structure is optically transparent. c, After melting the gelatin hydrogel, the remaining chitosan hydrogel can be picked up by a tweezer. The scale bar in a is 100 μm. The scale bar in b and c is 5 mm.

a crack appears and runs across the surface at a stretch about 1.6. With more stretch, more cracks progressively appear on the surface. At a stretch of 2, the chitosan layer is fractured into many small fragments (Fig. 7a). These cracks only take place in the chitosan layer rather than the polyacrylamide hydrogel, as the stretchability of the hydrogel is beyond 10. Each fragment is still strongly adhered with the hydrogel, as we cannot scratch a fragment off without breaking it. The force–stretch curve is measured and shows sawtooth-like behavior above a stretch of 1.64 (Fig. 7b). This is consistent with our observation, where the multiple force drops correspond to the multiple events of crack formation in the chitosan layer.

We design a control test to further ascertain that it is the chitosan layer, not the polyacrylamide hydrogel, that fractures during stretch. In the control test, the pH of the polyacrylamide hydrogel is tuned to 3 so that the chitosan topohesive cannot form a solid network. As expected, no crack forms on the surface of the chitosan–hydrogel bilayer for the entire course of stretching (Fig. 7c). The force–stretch curve is smooth without any sawtooth-like drops (Fig. 7d). The force level is almost a half lower than that measured in the former case with pH = 7 in the hydrogel. This implies that the chitosan layer in the former case carries a non-negligible force during the stretch of bilayer, even though the chitosan layer is one order of magnitude thinner than the hydrogel (∼100 μm vs. 1.5 mm). Furthermore, the load–unload curves for chitosan topohered polyacrylamide hydrogels of different pH show that a higher pH leads to a larger hysteresis (Figure S4), which indicates that a solid chitosan network formed at a high pH can dissipate more energy via multiple events of fractures, compared to a small viscous dissipation when chitosan chains do not form a network at a low pH.

We estimate the elastic modulus of the chitosan layer by comparing the two force–stretch curves. The elastic moduli are $E_{\text{bilayer}} = 9426$ Pa for the chitosan-polyacrylamide bilayer, and $E_{\text{gel}} = 4243$ Pa for the polyacrylamide hydrogel. The cross-sectional areas along the stretch direction are $A_{\text{chitosan}} = 2\times10^{-6}\text{m}^2$ for the chitosan layer, and $A_{\text{gel}} = 3\times10^{-5}\text{m}^2$ for the polyacrylamide hydrogel. Following the equation $E_{\text{gel}}A_{\text{gel}} + E_{\text{chitosan}}A_{\text{chitosan}} = E_{\text{bilayer}}(A_{\text{chitosan}} + A_{\text{gel}})$, we calculate $E_{\text{chitosan}} = 87{,}171$ Pa, one order of magnitude higher than E_{gel}. The stretchability of the chitosan layer is 1.6. The chitosan layer is a stiffer but more brittle hydrogel network compared to the polyacrylamide hydrogel.

We propose a mechanism of stretchable adhesion for the chitosan topohesive. After topohesion, the chitosan layer is in topological entanglement with two hydrogel networks (Fig. 8a). Under stretch, it fractures into islands (Fig. 8b). Unlike a rigid, non-stretchable interface formed by glassy polymers that can damage the adhered materials (for example, the elastic modulus

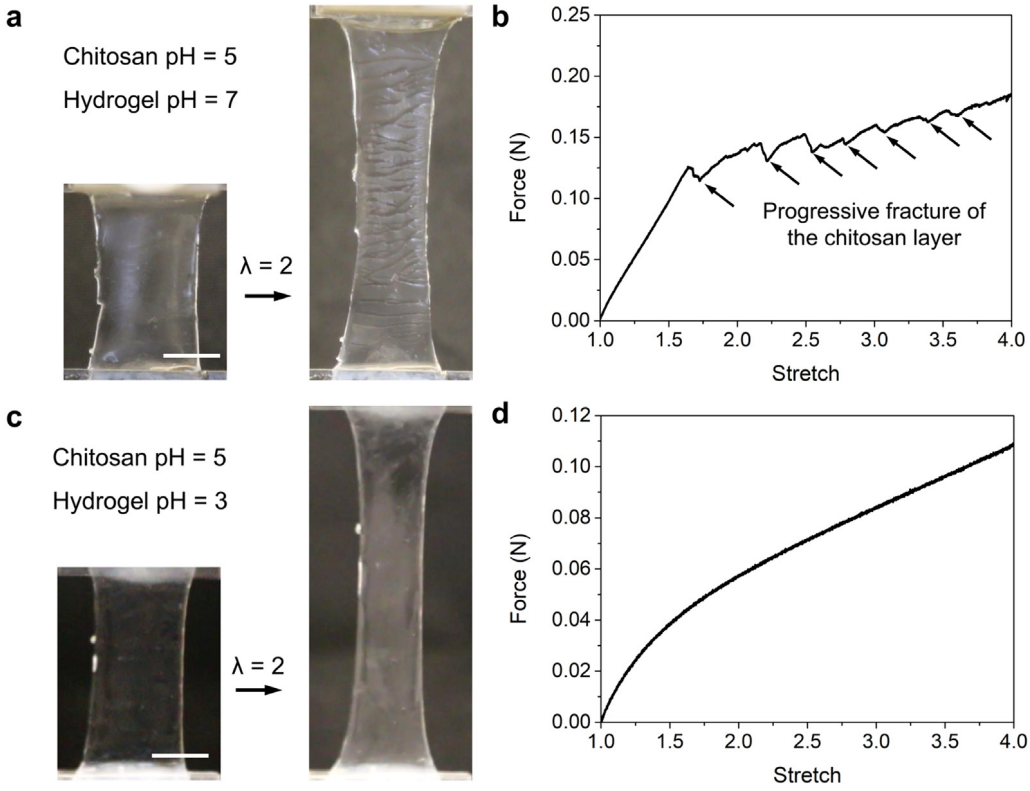

Fig. 7. Mechanical behavior of chitosan layer under stretch. a, Uniaxial test of a chitosan-hydrogel bilayer with the pH of the hydrogel is 7. The surface of the chitosan layer forms multiple cracks during stretch. b, The measured force–stretch curve shows sawtooth-like behavior. c, Uniaxial test of a chitosan-hydrogel bilayer when the pH of the hydrogel is 3. No crack is observed on the surface till the end of the stretch. d, The measured force–stretch curve is smooth. The scale bar in a and c is 1 cm.

of polycyanoacrylate is about 1 GPa [38]), the relatively low modulus of the chitosan layer (87,171 Pa) may not cause large strain concentration at the edges of the chitosan islands. Polymer chains in the chitosan islands can still deform, which may further break the islands into smaller pieces with increasing stretch. In the stretched state (e.g., stretch-hold tests), each chitosan island remains in topological entanglement with the two adherend networks, giving rise to strong adhesion. Upon removing the stretch, the chitosan islands follow the deformation and return to their undeformed state, maintaining the topological entanglement and preserving strong adhesion (Fig. 8c). Cyclic stretch repeats the above procedure, enabling strong adhesion independent with the numbers of cycles.

Beyond being stretchable, the interface should also be wet when adhering wet materials (i.e., tissues and hydrogels). The wet interface allows various species of molecules to transport across the interface from one wet material to the other. This feature is particularly important in biomedical applications as the wetness preserves biocompatibility and enhances tissue–device interactions. For example, therapeutic molecules from bioimplants can be delivered to tissues through the interface to treat diseases [36,39], and biofluids (e.g., sweat, tear) from tissues can diffuse through the interface to enable continuous biosensing [40–43]. In principle, interfacial wetness should be characterized for each adhesion system using molecule permeation test. In this test, one species of molecule markers is placed in one hydrogel, and the presence of the molecule markers in the other hydrogel is to be tested. A wet interface allows the molecules to diffuse across the interface, such that the molecule marker should be detected in the other hydrogel. In this paper, we do not characterize the wetness of the chitosan layer because the chitosan hydrogel is known to be wet, unlike adhesives such as cyanoacrylate.

The combination of interfacial wetness and mechanical robustness can stimulate numerous emerging innovations in biotechnology. For example, a cardiac patch glued on a beating heart that can maintain strong adhesion under millions of cycles and meanwhile deliver drugs or electric signals is ideal for chronic cardiac disease treatment; a wearable sensor attached on the skin that can withstand frequent body movements and simultaneously detect various chemicals in biofluids is desirable. In these applications, the stretchable interface not only ensures the conformal contact with the underlying tissues, but also prevent the tissue surfaces from damage.

Attaching backing layers can fix the deformation of test specimens in place. Inextensible backing layers such as glass and plastics are commonly used. However, such backing layers limit the choice of materials. In fact, so long as the modulus of a chosen material is orders of magnitude higher than that of the adherends and the material layer is also flexible to accommodate the T-peel adhesion test, it can be used as a backing layer. Such materials include stiff elastomers and hydrogels.

In summary, stretchable adhesion maintains strong adhesion while being deformed, or after deformation. We have demonstrated that topological adhesion of two hydrogels by chitosan topohesives is stretchable. The adhesion energy maintains at a similar level in all cases, despite different deformation histories or states of the hydrogels. We also propose the mechanism of chitosan enabled stretchable adhesion. The chitosan layer fractures into small islands under stretch, but remains in topological entanglement with the hydrogel networks, facilitating strong adhesion in the stretched state. Upon removing the stretch, the chitosan islands return to their undeformed state, still in topological entanglement with the hydrogel networks, and thus retaining the strong adhesion in the un-stretched state. Our study highlights the stretchability of the interface as an important design criterion

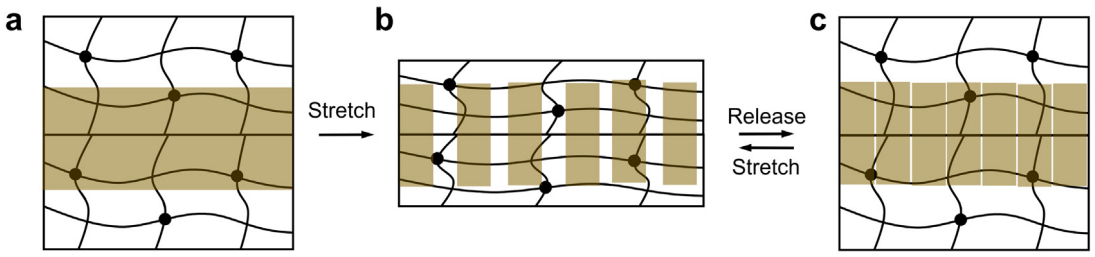

Fig. 8. Proposed mechanism of stretchable adhesion.

for soft materials adhesion. The testing methods to characterize stretchable adhesion are also useful for other adhesion systems and may be potential tools to study interfacial rheology.

Declaration of competing interest

The authors declare that they have no known competing financial interests or personal relationships that could have appeared to influence the work reported in this paper.

Acknowledgments

The work was supported by NSF MRSEC, USA (DMR-14-20570). J. Steck acknowledges the support from the National Science Foundation, USA Graduate Research Fellowship under Grant No. DGE1745303.

Appendix A. Supplementary data

Supplementary material related to this article can be found online at https://doi.org/10.1016/j.eml.2020.100891.

References

[1] K. Kendall, Molecular Adhesion and Its Applications: The Sticky Universe, Kluwer Academic Publishers, New York, 2004.
[2] A.J. Kinloch, Adhesion and Adhesives: Science and Technology, Cambridge: Chapman & Hall, 1987.
[3] S. Ebnesajjad, A.H. Landrock, Adhesives Technology Handbook, third ed., William Andrew, United States, 2014.
[4] C. Yang, Z. Suo, Hydrogel ionotronics, Nat. Rev. Mater. 3 (2018) 125–142.
[5] J. Yang, et al., Hydrogel adhesion: A supramolecular synergy of chemistry, topology, and mechanics, Adv. Funct. Mater. 30 (2) (2020) 1901693.
[6] P.J. Bouten, et al., The chemistry of tissue adhesive materials, Prog. Polym. Sci. 39 (7) (2014) 1375–1405.
[7] D. Wirthl, et al., Instant tough bonding of hydrogels for soft machines and electronics, Sci. Adv. 3 (6) (2017) e1700053.
[8] B. Chen, et al., Molecular staples for tough and stretchable adhesion in integrated soft materials, Adv. Healthc. Mater. 8 (19) (2019) 1900810.
[9] A.J. Singer, J.V. Quinn, J.E. Hollander, The cyanoacrylate topical skin adhesives, Am. J. Emerg. Med. 26 (4) (2008) 490–496.
[10] J. Li, et al., Tough adhesives for diverse wet surfaces, Science 357 (6349) (2017) 378–381.
[11] J. Yang, R. Bai, Z. Suo, Topological adhesion of wet materials, Adv. Mater. 30 (25) (2018) 1800671.
[12] X. Liu, et al., Hydrogel machines, Mater. Today (2020).
[13] H.R. Lee, C.C. Kim, J.Y. Sun, Stretchable ionics–A promising candidate for upcoming wearable devices, Adv. Mater. 30 (42) (2018) 1704403.
[14] H. Yuk, B. Lu, X. Zhao, Hydrogel bioelectronics, Chem. Soc. Rev. 48 (6) (2019) 1642–1667.
[15] Q. Liu, et al., Bonding dissimilar polymer networks in various manufacturing processes, Nat. Commun. 9 (1) (2018) 846.
[16] E. Acome, et al., Hydraulically amplified self-healing electrostatic actuators with muscle-like performance, Science 359 (6371) (2018) 61–65.
[17] N. Kellaris, et al., Peano-HASEL actuators: Muscle-mimetic, electrohydraulic transducers that linearly contract on activation, Sci. Robot. 3 (14) (2018) eaar3276.
[18] J.Y. Sun, et al., Ionic skin, Adv. Mater. 26 (45) (2014) 7608–7614.
[19] Z. Lei, et al., A bioinspired mineral hydrogel as a self-healable, mechanically adaptable ionic skin for highly sensitive pressure sensing, Adv. Mater. 29 (22) (2017).
[20] P. Le Floch, et al., Wearable and washable conductors for active textiles, ACS Appl. Mater. Interfaces 9 (30) (2017) 25542–25552.
[21] C.H. Yang, et al., Ionic cable, Extreme Mech. Lett. 3 (2015) 59–65.
[22] C. Keplinger, et al., Stretchable, transparent, ionic conductors, Science 341 (6149) (2013) 984–987.
[23] J. Yang, et al., Design molecular topology for wet–dry adhesion, ACS Appl. Mater. Interfaces 11 (27) (2019) 24802–24811.
[24] C.-C. Kim, et al., Highly stretchable, transparent ionic touch panel, Science 353 (6300) (2016) 682–687.
[25] H.R. Lee, et al., A stretchable ionic diode from copolyelectrolyte hydrogels with methacrylated polysaccharides, Adv. Funct. Mater. 29 (4) (2019) 1806909.
[26] C.H. Yang, et al., Electroluminescence of giant stretchability, Adv. Mater. 28 (22) (2016) 4480–4484.
[27] C. Larson, et al., Highly stretchable electroluminescent skin for optical signaling and tactile sensing, Science 351 (6277) (2016) 1071–1074.
[28] X. Liu, et al., Stretchable living materials and devices with hydrogel–elastomer hybrids hosting programmed cells, Proc. Natl. Acad. Sci. 114 (9) (2017) 2200–2205.
[29] X. Liu, et al., 3D printing of living responsive materials and devices, Adv. Mater. 30 (4) (2018) 1870021.
[30] N. Lang, et al., A blood-resistant surgical glue for minimally invasive repair of vessels and heart defects, Sci. Transl. Med. 6 (218) (2014) 218ra6.
[31] D.-A. Wang, et al., Multifunctional chondroitin sulphate for cartilage tissue–biomaterial integration, Nat. Mater. 6 (5) (2007) 385.
[32] S.Y. Chin, et al., Additive manufacturing of hydrogel-based materials for next-generation implantable medical devices, Sci. Robot. 2 (2) (2017) eaah6451.
[33] A. Meddahi-Pellé, et al., Organ repair, hemostasis, and in vivo bonding of medical devices by aqueous solutions of nanoparticles, Angew. Chem. Int. Ed. 53 (25) (2014) 6369–6373.
[34] Y. Yu, et al., Multifunctional "Hydrogel Skins" on diverse polymers with arbitrary shapes, Adv. Mater. (2018) 1807101.
[35] G.A. Parada, et al., Impermeable robust hydrogels via hybrid lamination, Adv. Healthc. Mater. 6 (19) (2017) 1700520.
[36] J. Li, D.J. Mooney, Designing hydrogels for controlled drug delivery, Nat. Rev. Mater. 1 (12) (2016) 16071.
[37] T.R. Hoare, D.S. Kohane, Hydrogels in drug delivery: Progress and challenges, Polymer 49 (8) (2008) 1993–2007.
[38] B. Mizrahi, et al., Elasticity and safety of alkoxyethyl cyanoacrylate tissue adhesives, Acta Biomater. 7 (8) (2011) 3150–3157.
[39] H. Yuk, et al., Dry double-sided tape for adhesion of wet tissues and devices, Nature 575 (7781) (2019) 169–174.
[40] J. Choi, et al., Skin-interfaced systems for sweat collection and analytics, Sci. Adv. 4 (2) (2018) eaar3921.
[41] J. Park, et al., Soft, smart contact lenses with integrations of wireless circuits, glucose sensors, and displays, Sci. Adv. 4 (1) (2018) eaap9841.
[42] X. Xie, et al., Reduction of measurement noise in a continuous glucose monitor by coating the sensor with a zwitterionic polymer, Nat. Biomed. Eng. 2 (12) (2018) 894.
[43] J. Wang, et al., Glucose-responsive insulin and delivery systems: Innovation and translation, Adv. Mater. 32 (13) (2020) 1902004.